An efficient simulation framework for prognostics of asymptotic processes- a case study in composite materials.

Manuel Chiachío[1], Juan Chiachío[2], Abhinav Saxena[3], Guillermo Rus[4], and Kai Goebel[5]

[1,2,4] *University of Granada, Non Destructive Evaluation Laboratory, Granada, 18071, Spain*
mchiachio@ugr.es
jchiachio@ugr.es
grus@ugr.es

[3,5] *NASA Ames Research Center, Intelligent Systems Division, Moffett Field, CA, 94035-1000, USA*
abhinav.saxena@nasa.gov
kai.goebel@nasa.gov

ABSTRACT

This work presents an efficient computational framework for estimating the *end of life* (EOL) and *remaining useful life* (RUL) by combining the particle filter (PF)-based prognostics with the technique of Subset simulation. It has been named PFP-SubSim on behalf of the full denomination of the computational framework, namely, *PF-based prognostics based on Subset Simulation*. This scheme is especially useful when dealing with the prognostics of evolving processes with asymptotic behaviors, as observed in practice for many degradation processes. The effectiveness and accuracy of the proposed algorithm is demonstrated through an example for predicting the probability density function of EOL for a carbon-fibre composite coupon subjected to an asymptotic fatigue degradation process. It is shown that PFP-SubSim algorithm is efficient, and at the same time, fairly accurate in obtaining the probability density function of EOL and RUL as compared to the traditional PF-based prognostic approach reported in the PHM literature.

1. INTRODUCTION

The goal of prognostics is to make end of life (EOL) and remaining useful life (RUL) predictions of components, subsystems, and systems that enable timely maintenance decisions to be made under the presence of uncertainty. In practice, different sources of uncertainty are present in a typical prognostic problem, namely, (a) uncertainty in modeling the system, (b) uncertainty in future inputs to the system and (c) measurements noise (Sankararaman & Goebel, 2013). Further it is added the uncertainty that the PF-based prognostics algorithm (Orchard, Kacprzynski, Goebel, Saha, & Vachtsevanos, 2008) introduces itself, since, in general, these prognostics algorithms employ a limited amount of discrete samples for making predictions, unless analytical methods are employed, which are limited to very specific cases in real life applications (Sankararaman & Goebel, 2013).

There is an additional source of error attributable to the prognostics algorithm itself, which is due to the lack of confidence in dealing with the EOL estimate, and it is especially representative of systems whose evolving dynamic exhibit an asymptotic behavior in approaching towards the thresholds. In this situation, prediction accuracy and precision can vary significantly unless higher-density sampling-based methods are employed to characterize fault propagation trajectories achieving higher resolutions in the vicinity of the threshold, which considerably increases the computational cost. On the other hand, choosing a conservative threshold, such that it meets a propagation trajectory prior to the asymptotic region, is one approach but results in throwing away potentially useful component life.

In this work, a novel efficient algorithm, named PFP-SubSim, is presented for estimating the EOL and RUL by combining the PF-based prognostics (Daigle & Goebel, 2011) with the technique of Subset simulation for efficient rare-event simulation, first developed in (Au & Beck, 2001). The result is a especially suited algorithm for the prognosis of asymptotic processes. The idea behind PFP-SubSim algorithm is to split the multi-step-ahead predicted trajectories into multiple branches of selected samples (seeds) at various stages of the process, which are further reproduced into closer approximations to the desired threshold by conditional sampling using the propagation model. A sequence of nested subsets of samples (*simulation levels*) are sequentially defined such that, at

each simulation level, the samples are increasingly distributed in the vicinity of the threshold, achieving high resolution for the EOL estimate.

A case study is presented for predicting the EOL of a composite coupon subjected to an asymptotic fatigue degradation process, that illustrates some of the challenges in a real-world application of the algorithm. Matrix micro-cracks are considered as the primary degradation mode where the increase in micro-cracks density exhibits asymptotic behavior as fatigue cycling continues. Structural health monitoring in this example is accomplished through Lamb wave-based active interrogation using PZT sensors together with a set of strain-gauges for measuring stiffness reduction. The data used for this case study is an open-access dataset distributed by NASA Ames Prognostics Data Repository (Saxena, Goebel, Larrosa, & Chang, 2008).

The paper is organized as follows. Section 2 reviews the theory underlying the prognostics problem and overviews the computational architecture we adopt in further sections. In Section 3 the basis of Subset Simulation method is presented before introducing a formal Subset Simulation approach in a prognostic context, which is provided in Section 4. The efficiency of FPF-SubSim is illustrated in Section 5 through a case study. In Section 6, a discussion about the performance of PFP-SubSim algorithm in relation with the standard PF-based prognostic algorithm is provided. Section 7 provides concluding remarks.

2. PF-BASED PROGNOSTICS

Let consider a state-space model which is used to sequentially predicting the state $x_k \in \mathcal{X} \subset \mathbb{R}^{n_x}$ of a dynamic system for observed data vector y_k, where $k \in \mathbb{N}$, is the time index. Let us also consider that the state x_k may depends on a set of model parameters $\theta \in \mathbf{\Theta} \subset \mathbb{R}^{n_\theta}$. Mathematically, the state-space model can be described at time k in a generalized manner as:

$$x_k = f_k(x_{k-1}, u_k, v_k, \theta) \tag{1a}$$

$$y_k = h_k(x_k, u_k, w_k, \theta) \tag{1b}$$

where $u_k \in \mathbb{R}^{n_u}$ is the input vector and $v_k \in \mathbb{R}^{n_v}$ and $w_k \in \mathbb{R}^{n_w}$, are uncertain variables introduced to account for the model error and measurement error, respectively. The functions f_k and h_k are possibly nonlinear functions for the state transition evolution and observation equation, respectively. In the last equation, the measurements y_k are assumed conditionally independent given the parameter $\theta \in \mathbb{R}^{n_\theta}$ and the states $x_k \in \mathcal{X}$, follow a Markov model of order one. In addition, it is defined the augmented state z_k in the joint state-parameter space as $z_k = (x_k, \theta) \in Z = \mathbf{\Theta} \times \mathcal{X} \subset \mathbb{R}^{n_\theta + n_x}$, so that $p(z_k) = p(x_k|\theta)p(\theta)$. The focus of state-estimation (also known as the *filtering problem*) is on sequentially updating the probability density function (PDF) of the state z_k, given the observed measurements up to time k, $y_{0:k} = \{y_0, \ldots, y_{k-1}, y_k\}$, i.e., $p(x_k, \theta_k|y_{0:k}) \equiv p(z_k|y_{0:k})$. This implies the evaluation of multidimensional integrals parameterized by θ, within a Bayesian framework of prediction and updating (Cappe, Guillin, Marin, & Robert, 2004). These integrals are usually intractable except some especial cases of linear systems and Gaussian noise, hence a generally followed solution is to obtain an approximation to $p(z_k|y_{0:k})$ by means of *particle filters* (PF) (Gordon, Salmond, & Smith, 1993), which may be directly applied to nonlinear systems with non-Gaussian noise terms (Arulampalam, Maskell, Gordon, & Clapp, 2002). Using PF, the approximation to the state distribution $p(z_k|y_{0:k})$ is described through a set of N discrete weighted *particles* $\left\{(x_k^{(i)}, \theta_k^{(i)}, \omega_k^{(i)}\right\}_{i=1}^N$ that can be readily sampled from a convenient importance distribution $q(x_{0:k}, \theta_{0:k}|y_{0:k})$ as:

$$p(x_{0:k}, \theta_{0:k}|y_{0:k}) \approx \sum_{i=1}^{N} \hat{w}_k^{(i)} \delta(x_{0:k} - x_{0:k}^{(i)}) \delta(\theta_{0:k} - \theta_{0:k}^{(i)}) \tag{2}$$

where $\hat{w}_k^{(i)}$ is the unnormalized importance weight for the ith particle:

$$\hat{w}_k^{(i)} = \frac{p(x_{0:k}^{(i)}, \theta_{0:k}|y_{0:k})}{q(x_{0:k}^{(i)}, \theta_{0:k}|y_{0:k})} \tag{3}$$

For practical reasons, the PDF $q(x_{0:k}, \theta_{0:k}|y_{1:k})$ is chosen so that it admits a sample procedure by choosing $q(x_{0:k}, \theta_{0:k}|y_{0:k}) = q(x_{0:k}, \theta_{0:k}|y_{0:k-1})$ (Arulampalam et al., 2002), hence it can be factorized in a form similar to that of the target posterior PDF, i.e. :

$q(x_{0:k}, \theta_{0:k}|y_{0:k}) = q(x_{0:k-1}, \theta_{0:k-1}|y_{0:k-1}) q(x_k|x_{k-1}, \theta_{k-1})$, resulting:

$$\hat{w}_k^{(i)} \propto \hat{w}_k^{(i-1)} \frac{p(x_k^{(i)}|x_{k-1}^{(i)}, \theta_{k-1}^{(i)}) p(y_k|x_k^{(i)}, \theta_k^{(i)})}{q(x_k^{(i)}|x_{k-1}^{(i)}, \theta_k^{(i)})} \tag{4}$$

where $p(x_k^{(i)}|x_{k-1}^{(i)}, \theta_{k-1}^{(i)})$ and $p(y_k|x_k^{(i)}, \theta_k^{(i)})$ are[1] the PDFs of state estimation and updating, respectively, which can be obtained using the state-space model defined in Eq. (1) and assuming prescribed PDFs for v_k and w_k. Without lack of generality, we adopt the *bootstrap filter* (Gordon et al., 1993) consisting on adopting $q(x_k|x_{k-1}, \theta_{k-1}) = p(x_k|x_{k-1}, \theta_{k-1})$, so that the expression for the ith unnormalized particle weight yields

$$\hat{w}_k^{(i)} \propto \hat{w}_{k-1}^{(i)} p(y_k|x_k^{(i)}, \theta_k^{(i)}) \tag{5}$$

Observe from Eqs. (4) and (5) that the weight values $\hat{w}_k^{(i)}$ are known only up to a scaling factor, which can be overpassed by normalization as: $w_k^{(i)} = \hat{w}_k^{(i)} / \sum_{i=1}^N \hat{w}_k^{(i)}$, $i = 1, \ldots, N$, where $w_k^{(i)}$ denotes the normalized value of the ith particle

[1]For simpler notation the conditioning on the model input u_k is dropped from Eq. (1)

at time k. A pseudocode implementation of the PF is given in Algorithm 1, which includes a systematic resampling step (Rubin, 1987) to avoid the well-known degeneracy deficiency of the PF (Cappe et al., 2004).

2.1. Prognostics and RUL prediction

Prognostics is concerned with the performance of the component that lies outside a given region of acceptable behavior. Mathematically, it requires the generation of a ℓ-step ahead prediction of state PDF, namely $p(z_{k+\ell}|y_{1:k})$, using the most up-to-date knowledge of the system at time k (Orchard et al., 2008). By computing the time indexes $t > k \in \mathbb{N}$ when future states z_t violate any previously defined thresholds, an estimate of the end of life (EOL) can be derived.

Algorithm 1 PF with on-line parameter updating

inputs:
N, {number of particles per time step}
Algorithm:
Initialize $\left[\left(\theta_0^{(1)}, x_0^{(1)}\right), \ldots, \left(\theta_0^{(i)}, x_0^{(i)}\right), \ldots, \left(\theta_0^{(N)}, x_0^{(N)}\right)\right]$, where $(\theta, x) \sim p(\theta)p(x|\theta)$
Assign the initial unnorrmalized weights: $\left\{\hat{w}_0^{(i)} = p(y_0|x_0^{(i)}, \theta^{(i)})\right\}_{i=1}^N$
At $k \geqslant 1$ {time k evolves as new data point arrives}
Resampling of N particles according to weights $w_{k-1}^{(i)}, i = 1, \ldots, N$.
for $i = 1$ to N **do**
  Sample: $\theta_k^{(i)} \sim p(\theta_k|\theta_{k-1}^{(i)})$
    $x_k^{(i)} \sim p(x_k|x_{k-1}^{(i)}, \theta_k^{(i)})$.
  Update the weight $\hat{w}_k^{(i)} = p(y_k|x_k^{(i)}, \theta_k^{(i)})$
end for
Normalize weights $w_k^{(i)} = \hat{w}_k^{(i)} / \sum_{i=1}^N \hat{w}_k^{(i)}$
output: $\left\{(x_k^{(i)}, \theta_k^{(i)}), w_k^{(i)}\right\}_{i=1}^N$

The region of unacceptable behavior can be defined by means of a set of thresholds $\mathbf{b} = \{b_1, \ldots, b_c\}$ on one or various critical parameters. These thresholds can be combined into a *threshold function* $T_{EOL} = T_{EOL}(x, \theta) \equiv T_{EOL}(z)$, that maps a given point in the joint state-parameter space to the Boolean domain $\{0, 1\}$ (Daigle & Goebel, 2011). For instance, when a given particle i starting from time k performs a random walk and hits any of the thresholds in $\mathbf{b}$, then $T_{EOL}^{(i)} \equiv T_{EOL}(z_k^{(i)}) = 1$, otherwise $T_{EOL}^{(i)} = 0$. The time $t \geqslant k$ at which that happens defines the EOL_k for that particle. Mathematically:

$$EOL_k^{(i)} = \inf\{t \in \mathbb{N} : t \geqslant k \wedge T_{EOL}^{(i)} = 1\} \tag{6}$$

Using the updated weights at the starting time k, an approximation to the PDF of EOL is given by:

$$p(EOL_n|y_{0:k}) \approx \sum_{i=1}^N \omega_k^{(i)} \delta(EOL_k - EOL_k^{(i)}) \tag{7}$$

Once EOL_n is estimated, the remaining useful life can be readily obtained as $RUL_k = EOL_k - k$. An algorithmic description of the prognostic procedure is provided as Algorithm 2.

Algorithm 2 Standard PF-prognostics and RUL prediction

inputs: $\left\{\left(x_k^{(i)}, \theta_k^{(i)}\right), \omega_k^{(i)}\right\}_{i=1}^N$, $\mathbf{b} = \{b_1, \ldots, b_c\}$
for $i = 1 \to N$ **do**
  Calculate: $T_{EOL}\left(x_k^{(i)}, \theta_k^{(i)}\right)$
  while $T_{EOL}^i = 0$ **do**
    Sample: $\theta_t^{(i)} \sim p(\theta_t|\theta_{t-1}^{(i)})$
      $x_t^{(i)} \sim p(x_t|x_{t-1}^{(i)}, \theta_t^{(i)})$.
    $t \leftarrow t + 1,\ t > k$
    $z_t = \left(x_t^{(i)}, \theta_t^{(i)}\right) \leftarrow z_{t+1} = \left(x_{t+1}^{(i)}, \theta_{t+1}^{(i)}\right)$
  end while
  $EOL_k^{(i)} \leftarrow t$
  $RUL_k^{(i)} = EOL_k^{(i)} - k$
end for
output $EOL_k,\ RUL_k = EOL_k - k$

3. SUBSET SIMULATION METHOD

Subset Simulation is an adaptive stochastic simulation approach originally proposed to compute small failure probabilities of engineering systems (Au & Beck, 2001). The conceptual idea behind Subset Simulation is to represent a small failure probability as a product of larger probabilities.

In a general way, Subset Simulation is a method for efficiently generating conditional samples that correspond to specified levels of a performance function $g : \mathbb{R}^{n_\theta + n_x} \to \mathbb{R}$ in a progressive manner, converting a problem involving rare-event simulation into a sequence of problems involving more frequent events. This general aspect makes Subset Simulation applicable to a broad range of areas of science where the simulation/prediction of unprovable events is required (Au & Beck, 2003; Ching, Au, & Beck, 2005). In this section, the Subset Simulation method is presented using its primary aim on small failure probabilities estimation. In the next section, Subset Simulation is specialized for the use in prognostics, and in particular for asymptotic processes.

Let $\mathcal{F}$ be the region of unacceptable behavior, or failure region, in the z-space, $z \in Z \subset \mathbb{R}^{n_\theta + n_x}$, corresponding to exceedance of the performance function g above some specified threshold level b:

$$\mathcal{F} = \{z \in Z : g(z) > b\} \tag{8}$$

Let us now assume that $\mathcal{F}$ is defined as the intersection of m regions Z, i.e, they are arranged as nested subsets of regions starting from the entire space Z and shrinking to the failure domain $\mathcal{F}$, i.e., $\mathcal{F}_1 \supset \mathcal{F}_2 \ldots \supset \mathcal{F}_{m-1} \supset \mathcal{F}_m = \mathcal{F}$, so that $\mathcal{F} = \bigcap_{j=1}^{m} \mathcal{F}_j$. Each subset $\mathcal{F}_j$ (typically termed as *intermediate failure domain*) is defined as $\mathcal{F}_j = \{z \in Z : g(z) > b_j\}$, with $b_{j+1} > b_j$, such that $p(z|\mathcal{F}_j) \propto p(z)\mathbb{I}_{\mathcal{F}_j}(z)$, $j = 1, \ldots, m$. The term $p(z)$ denotes the probability model for z. By definition of conditional probability, it follows that[2]:

$$P(\mathcal{F}) = P\Big(\bigcap_{j=1}^{m} \mathcal{F}_j\Big) = P(\mathcal{F}_1) \prod_{j=2}^{m} P(\mathcal{F}_j|\mathcal{F}_{j-1}) \quad (9)$$

where $P(\mathcal{F}_j|\mathcal{F}_{j-1}) \equiv P(z \in \mathcal{F}_j | z \in \mathcal{F}_{j-1})$, is the conditional failure probability at the $(j-1)^{th}$ intermediate failure domain. Observe that the probability $P(\mathcal{F})$ may be relatively small, however it can be approximated by Subset Simulation as the product of larger conditional probabilities involved in Eq. (9), thus avoiding simulation of rare events.

In the last equation, apart from $P(\mathcal{F}_1)$, which can be readily estimated by the standard Monte Carlo method (MC), the remaining factors cannot be efficiently estimated because of the sampling conditional on $\mathcal{F}_{j-1}$, $j = 2, \ldots, m$. However, MCMC methods can be used for sampling from the PDF $p(z_{j-1}|\mathcal{F}_{j-1})$ when $j \geqslant 2$ giving:

$$P(\mathcal{F}_j|\mathcal{F}_{j-1}) \approx \bar{P}_j = \frac{1}{M} \sum_{n=1}^{M} \mathbb{I}_{\mathcal{F}_j}(z_{j-1}^{(n)}) \quad (10)$$

where $z_{j-1}^{(n)} \sim p(z_{j-1}|\mathcal{F}_{j-1})$ and $\mathbb{I}_{\mathcal{F}_j}(z_{j-1}^{(n)})$ is an indicator function for the region $\mathcal{F}_j, j = 1, \ldots, m$, that assigns a value of 1 when $g(z_{j-1}^{(n)}) > b_j$, and 0 otherwise.

Observe that it is possible to obtain Markov chain samples that are generated at the $(j-1)^{th}$ level which lie in $\mathcal{F}_j$, so that they are distributed as $p(z|\mathcal{F}_j)$. Hence they provide "seeds" for simulating more samples according to $p(z|\mathcal{F}_j)$ by using MCMC sampling with no burn-in required, which is an important feature of Subset Simulation to avoid wasting samples (Au & Beck, 2001). As described further below, $\mathcal{F}_j$ is actually chosen adaptively based on the samples $\{z_{j-1}^{(n)}, n = 1, \ldots, M\}$ from $p(z|\mathcal{F}_{j-1})$ in such a way that the worst (in the sense of closer to the intermediate failure threshold) among the M samples define an intermediate level. For practical reasons, the amount of samples defining the intermediate level are chosen as a specified fraction of the total amount of M samples by fixing a value $P_0 \in (0, 1)$, so that there are exactly NP_0 of these seed samples in $\mathcal{F}_j$ $\big($so $\bar{P}_j = P_0$ in Eq. (10)$\big)$. For a specified value of P_0, the intermediate threshold value b_j defining $\mathcal{F}_j$ is obtained in an adaptive manner as the $[MP_0]^{th}$ largest value among the values $g(z_{j-1}^{(n)})$, $n = 1, \ldots, M$, so that the sample estimate of $P(\mathcal{F}_j|\mathcal{F}_{j-1})$ in Eq. (10) is equal to P_0. The remaining $M(1 - P_0)$ samples are generated from $p(z|\mathcal{F}_j)$ by MCMC, giving a total of M samples in $\mathcal{F}_j$. Repeating this process, we can compute the conditional probabilities of the higher-conditional levels until the final region $\mathcal{F}_m = \mathcal{F}$ has been reached.

In Subset Simulation, the choice of an adequate P_0 has a significant impact on the efficiency of the algorithm. Indeed, a small value for the conditional probability ($P_0 \to 0$) makes that the distance between consecutive intermediate levels $b_j - b_{j-1}$ becomes too large, which leads to a rare-event simulation problem. In the other hand, if the intermediate threshold values were chosen too close ($P_0 \to 1$), the algorithm would take a large total number of simulation levels m (and hence large computational effort) to progress toward the target region of interest, $\mathcal{F}$. Hence, a rational choice for P_0 is of key importance for the efficiency of the algorithm. In the original presentation of Subset Simulation in (Au & Beck, 2001), $P_0 = 0.1$ was recommended, and more recently in (Zuev, Beck, Au, & Katafygiotis, 2011), the range $0.1 \leqslant P_0 \leqslant 0.3$ was found to be near optimal after a rigorous sensitivity study of Subset Simulation. In this paper, we will adopt $P_0 = 0.2$. For convenience of implementation, P_0 is chosen so that MP_0 and $1/P_0$ are positive integers.

As stated before, to draw samples from the target PDF $p(z|\mathcal{F}_j)$, MCMC methods like Metropolis-Hastings (Metropolis, Rosenbluth, Rosenbluth, Teller, & Teller, 1953) are adequate. In the original version of Subset Simulation (Au & Beck, 2001), a modified Metropolis algorithm (MMA) was proposed that worked well even in very high dimensions (e.g. 10^3-10^4), because the original algorithm fails in this case (Au & Beck, 2001)). In MMA, a univariate proposal PDF is chosen for each component of the parameter vector and each component candidate is accepted or rejected separately, instead of drawing a full parameter vector candidate from a multi-dimensional PDF as in the original algorithm. To avoid repeating literature, the reader is refered to (Au & Beck, 2001) for further details about MMA. More details about implementation issues can be encountered in the work of (Zuev et al., 2011).

4. SUBSET SIMULATION IN PF-BASED PROGNOSTICS

In this section, the Subset Simulation method presented above is adapted for its application in prognostics. The definition of failure region $\mathcal{F}$ in Eq. (8) is adopted here to establish a nested sequence of prognostic regions $\mathcal{F}_j$ in $Z = \boldsymbol{\Theta} \times \mathcal{X}$, whose points are of the form $z_t^j \equiv (x_t^j, \theta_t^j)$, $t > k$, such that $g(z_t^j) < b_j$, being $g : \mathcal{F} \to \mathbb{R}$ the performance function on Z. The sequence of threshold values $b_{j+1} > b_j$, $j = 1, \ldots, m$ are

[2]In what follows, we use $P(\cdot)$ to denote probability whereas a PDF is expressed as $p(\cdot)$. In addition, we use $P(\mathcal{F}) \equiv P(z \in \mathcal{F})$, for simpler notation

obtained[3] sequentially as in Section 3. Observe that the performance function g works analogously to the T_{EOL} function defined in Section 2.1. The main difference between them is that g allows us to know not only whether the state has reached the threshold b, but also how close it is to b if it has not.

Summarizing, the proposed algorithm simulate sequentially the joint state-parameter $z_t^j = (x_t^j, \theta_t^j)$ over a set of nested regions $\mathcal{F}_j,\ j = 1, \ldots, m$, such that $z_t^j \sim \mathbb{I}_{\mathcal{F}_j}(\theta, x)p(x|\theta)p(\theta)$. Figure 1 schematically describes the performance of the algorithm.

See Algorithm 3 for a pseudocode implementation, which is intended to be sufficient for most cases of application. The algorithm is implemented such that a fixed amount of M samples are drawn per simulation level $\mathcal{F}_j$, so that $N_T = mM$: the total amount of model evaluations required by the algorithm to reach the final threshold. It is important to remark that it does not imply any restriction but it allows controlling the computational burden. In addition, the conditional probability is set to $P_0 = 0.2$, following the recommendation about Subset Simulation method in (Zuev et al., 2011). Figure 2 provides an algorithm flow-chart to better understand the main steps of the algorithm. For simplicity, the time subscripts are dropped from Step 10, since the time indexing information is implicitly contained at each sample.

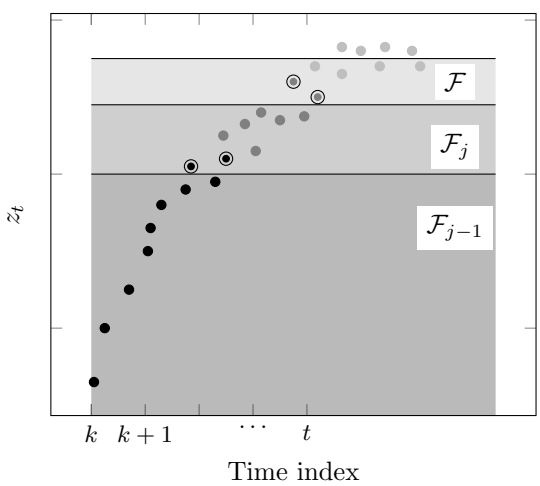

Figure 1. Generation of conditional samples in PFP-SubSim: solid disks represent samples in the joint state-parameter space. Darker gray tones are used to represent samples distributed in increasing intermediate regions. Circled disks are the Markov chain samples used as seeds for generating new samples distributed as $p(\cdot|\mathcal{F}_j),\ j = 1, \ldots, m$.

[3]The b_j sequence is an increasing sequence (i.e., $b_{j+1} > b_j$) or a decreasingly sequence ($b_{j+1} < b_j$) depending wether the process is a non-decreasing or decreasing process, respectively. With no loss of generality, it is considered as an increasing sequence.

Algorithm 3 Pseudocode implementation for PFP-SubSim

1: **Inputs:**
2: $P_0 \in [0, 1]$ {gives percentile selection, chosen so $NP_0, {}^1/_{P_0} \in \mathbb{Z}^+$; $P_0 = 0.2$ is recommended}.
3: M, {number of samples per intermediate level}; m, {maximum number of simulation levels allowed}; $\ell = M/N$.

Require: $\{(x_k^{(i)}, \theta_k^{(i)}), w_k^{(i)}\}_{i=1}^N$; e.g. use Algorithm 1.

4: **Algorithm:**
5: **for** $i : 1, \ldots, N$ **do**
6: **for** $t : k+1, \ldots, k+\ell$ **do**
7: Sample $\theta_t^{0,(i)} \sim p(\theta_t|\theta_{t-1}^{(i)})$
$x_t^{0,(i)} \sim p(x_t|x_{t-1}^{(i)}, \theta_t^{(i)})$.
8: **end for**
9: **end for**
10: $\left[(\theta^{0,(1)}, x^{0,(1)}), \ldots, (\theta^{0,(M)}, x^{0,(M)})\right]$
11: **for** $j : 1, \ldots, m$ **do**
12: **for** $n : 1, \ldots, M$ **do**
13: Evaluate: $g_j^{(n)} = g\big(z^{j-1,(n)}\big)$;
14: **end for**
15: Sort $\left[\big(\theta^{j-1,(n)}, x^{j-1,(n)}\big), n : 1, \ldots, M\right]$ so that $g_j^{(1)} \leqslant g_j^{(2)} \leqslant \ldots g_j^{(M)}$
16: Fix $b_j = \frac{1}{2}\left(g_j^{(MP_0)} + g_j^{(MP_0+1)}\right)$
17: **for** $n = 1, \ldots, MP_0$ **do**
18: Select as a seed $\big(\theta_{(1)}^{j,(n)}, x_{(1)}^{j,(n)}\big) = \big(\theta^{j-1,(n)}, x^{j-1,(n)}\big) \sim p\big(\theta, x|\mathcal{F}_j\big)$
19: Run MMA (Au & Beck, 2001) to generate $1/P_0$ states of a Markov chain lying in $\mathcal{F}_j$: $\left[\big(\theta_{(1)}^{j,(n)}, x_{(1)}^{j,(n)}\big), \ldots, \big(\theta_{(1/P_0)}^{j,(n)}, x_{(1/P_0)}^{j,(n)}\big)\right]$
20: **end for**
21: Renumber $\left[\big(\theta_{(i)}^{j,(n)}, x_{(i)}^{j,(n)}\big)\right]$
$n = 1, \ldots, MP_0;\ i = 1, \ldots, 1/P_0$ as:
22: $\left[(\theta^{j,(1)}, x^{j,(1)}), \ldots, (\theta^{j,(M)}, x^{j,(M)})\right]$
23: **if** $b_j \geqslant b$ **then**
Record the times indexes of the first-passage points→End Algorithm
24: **end if**
25: **end for**

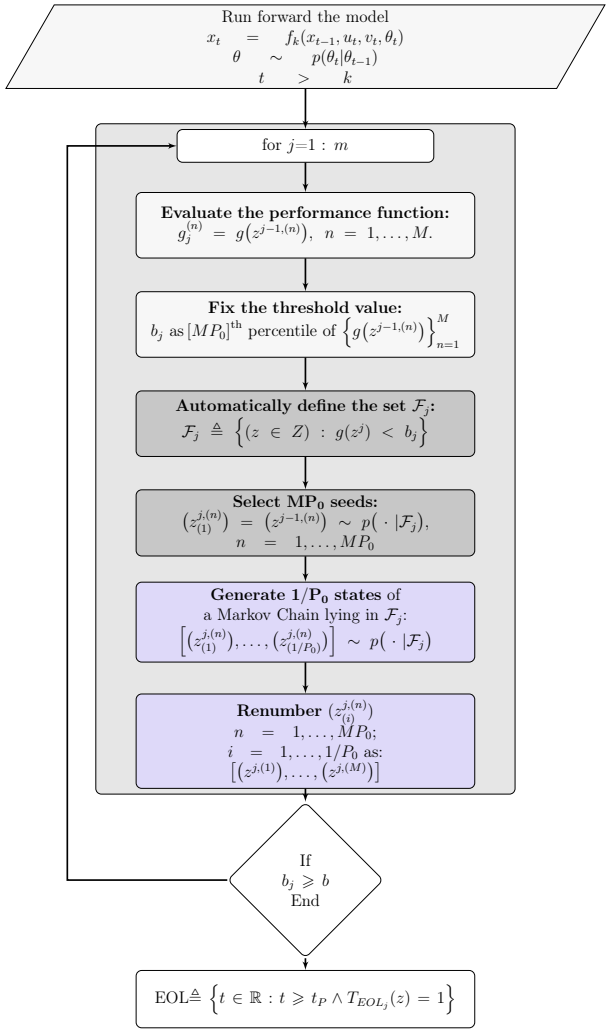

Figure 2. PFP-SubSim algorithm flowchart.

5. CASE STUDY

In this section, the performance of the algorithm is investigated on a challenging problem about prognostics of matrix micro-cracks saturation in CFRP laminates using SHM data from a fatigue experiment. The framework for prognostics of fatigue damage in CFRP composites has been recently contributed by the authors in (Chiachío, Chiachío, Saxena, Rus, & Goebel, 2013) and (Chiachío, Chiachío, Saxena, Rus, & Goebel, 2013). To avoid repeating literature but conferring a sufficient conceptual framework, the relevant details are presented here in a brief manner.

5.1. Damage modeling in composites

As already shown in (Chiachío et al., 2013), a physic-based prognostic framework is preferred as a versatile way to deal with accurate predictions for fatigue damage in composites without much training. It is based on modeling the energy released per unit crack area due to the formation of a new crack between two existing cracks, denoted as G. This energy, known as energy release rate (ERR), can be obtained as (J. A. Nairn, 1989, 1995):

$$G = \frac{\sigma_x^2 h}{2\rho h_{90}} \left(\frac{1}{E_x^*(2\rho)} - \frac{1}{E_x^*(\rho)} \right) \tag{11}$$

where σ_x is the maximum applied axial tension to the laminate, ρ is the matrix micro-cracks density defined as $\rho = \frac{1}{2\bar{l}}$ with $\bar{l}$ being the normalized half-crack spacing, and h and h_{90} are the laminate and 90°-sublaminate half-thickness, respectively. See more details in the Nomenclature section. The term $E_x^*(\rho)$, as a function of ρ, is the effective longitudinal laminate stiffness, i.e. the stiffness due to the current damage state, which can be efficiently modeled through micro-damage mechanics models like *shear-lag* models (Garrett & Bailey, 1977; Highsmith & Reifsnider, 1982), *variational* models (Hashin, 1985), and *crack opening displacement* based models (Gudmundson & Weilin, 1993; Lundmark & Varna, 2005). In this work, the shear-lag approach is adopted for being simpler and well-suited for symmetric cross-ply laminates, which is the laminate type used in this case study, as shown below. Equation (12) provides the analytical expression for the effective longitudinal stiffness using the classical shear-lag model (Joffe & Varna, 1999):

$$E_x^* = \frac{E_{x,0}}{1 + a\frac{1}{2\bar{l}}R(\bar{l})} \tag{12}$$

In the last equation, $E_{x,0}$ is the intact longitudinal Young's modulus of the laminate, $\bar{l} = \frac{l}{h_{90}}$ is the half crack-spacing normalized with the 90° sub-laminate thickness and a is a known function of laminate properties (defined in the Appendix). The function $R(\bar{l})$, known as the *average stress perturbation function*, is defined by:

$$R(\bar{l}) = \frac{2}{\xi} \tanh(\xi \bar{l}) \tag{13}$$

where ξ is the shear-lag parameter which is expressed as a function of ply and laminate properties (see the Nomenclature section for further details about the terms involved in the next expression) as:

$$\xi^2 = G_{yz} \left(\frac{1}{E_y} + \frac{1}{\lambda E_x^{(\phi)}} \right) \tag{14}$$

The evolution of crack-density over time is achieved by introducing the ERR into the modified Paris' law (J. Nairn & Hu, 1992), as shown below:

$$\frac{\mathrm{d}\rho}{\mathrm{d}n} = A(\Delta G)^{\alpha} \tag{15}$$

In the last equation, A and α are fitting parameters and ΔG is the increment in ERR for a specific stress amplitude during the fatigue loading: $\Delta G = G(\sigma_{x,max}) - G(\sigma_{x,min})$. Due to the complexity of the expression for ΔG, which involves the underlying micro-damage mechanics model for the computation of $E_x^*(\rho)$ shown above, a closed-form solution for Eq. (15) is hard to obtain. To overcome this drawback, the resulting differential equation can be solved by approximating the derivative using "unit-time" finite differences, considering that damage evolves cycle-to-cycle, as:

$$\rho_n = \rho_{n-1} + A\left(\Delta G(\rho_{n-1})\right)^{\alpha} \tag{16}$$

5.2. Filtering recursion

As discussed in the last section, the progression of damage is modeled at every cycle n by focusing on the matrix-cracks density, ρ_n, and the normalized effective stiffness, $D_n = \frac{E_x^*}{E_{x,0}}$, defining a joint response function of two components: $f_n = [f_{1_n}, f_{2_n}]$ for matrix cracks-density and normalized effective stiffness, respectively. Let denote by $x_n = [x_{1_n}, x_{2_n}]$ the actual system response, for matrix micro-cracks density and normalized effective stiffness, respectively. Next, the damage model can be embedded stochastically (Beck, 2010) by adding a model-error term $v_n \in \mathbb{R}^2$ that represents the difference between the actual system response x_n and the model output f_n. The following input/output (I/O) state-space model is defined:

$$x_{1_n} = \rho_n = \underbrace{f_{1_n}(\rho_{n-1}, \theta, u_n)}_{\text{Equation 16}} + v_{1_n} \tag{17a}$$

$$x_{2_n} = D_n = \underbrace{f_{2_n}(\rho_n, \theta, u_n)}_{\text{Equation 12}} + v_{2_n} \tag{17b}$$

where θ is a set of updatable model parameters and u_n denotes the set of input parameters to the system at time n. If $y_n = [y_{1_n}, y_{2_n}] = \left[\hat{\rho}_n, \hat{D}_n\right]$ are the measurements of the system output x_n, then the following measurement function is added to the discrete state-space model to account for the measurement error $w_n \in \mathbb{R}^2$:

$$y_{1_n} = \hat{\rho}_n = x_{1_n} + w_{1_n} \tag{18a}$$

$$y_{2_n} = \hat{D}_n = x_{2_n} + w_{2_n} \tag{18b}$$

We use the Principle of Maximum Information Entropy (Beck, 2010) to choose v_n and w_n as i.i.d. Gaussian variables, $v_n \sim \mathcal{N}(0, \left[\sigma_{v_{1_n}}, \sigma_{v_{2_n}}\right] I_2)$, $w_n \sim \mathcal{N}(0, \left[\sigma_{w_{1_n}}, \sigma_{w_{2_n}}\right] I_2)$, being $\left[\sigma_{v_{1_n}}, \sigma_{v_{2_n}}\right]$ and $\left[\sigma_{w_{1_n}}, \sigma_{w_{2_n}}\right]$ the standard deviations of v_n and w_n respectively, and I_2 the identity matrix of order 2, so they can be readily sampled. For this example, we adopt $\sigma_{w_{1_n}} = 10^{-2}$ and $\sigma_{w_{1_n}} = 10^{-6}$, assuming as known. The model parameters θ are selected among the complete set of parameters that defines the ensemble based on the modified Paris' law through a global sensitivity analysis based on variances and following the methodology proposed by (Saltelli et al., 2008). As result, the ply properties $\{E_x, E_y, h\}$ together with the modified Paris' law fitting parameter $\{\alpha\}$ emerged as influential parameters in terms of model output uncertainty. Moreover, the set of updatable model parameters θ was completed by adding the error terms to the last choice, i.e., $\boldsymbol{\theta} = \{\alpha, E_x, E_y, h, \sigma_v, \sigma_w\}$. The rest mechanical and geometrical parameters act as static non-updatable input parameters, hence they can be readily fixed at any point within their range of variation, (e.g. the mean value) without significantly influencing the output uncertainty.

5.3. Dataset

The performance of the proposed algorithm is investigated using SHM data obtained from a set of run-to-failure fatigue experiments. Both stiffness data and NDE measurements of internal damage, such as micro-crack density and delamination area, were periodically measured during the fatigue test (Saxena et al., 2011) (although we will only focus here on predicting matrix-micro cracks). Torayca T700G uni-directional carbon-prepreg material was used for $15.24\ cm \times 25.4\ cm$ coupons with notched dogbone geometry and stacking sequence defined by $[0_2/90_4]_s$. The nominal values of the laminate ply properties are given in Table 1, along with their statistical description.

The tests were conducted under load-controlled tension cyclic loading, with a maximum applied load of 31.13 KN, frequency $f = 5$ Hz, and a stress ratio $R = 0.14$ (defined as the relation between the minimum and maximum stress for each cycle). Lamb wave signals were periodically recorded using a PZT sensor network to estimate internal micro-crack density. The mapping between PZT raw data and micro-crack density was done following the methodology proposed in (Larrosa & Chang, 2012). Additionally, periodic X-rays were taken to visualize and characterize subsurface damage features, in particular, the micro-crack damage pattern. More details about these tests are reported in the Composite dataset, NASA Ames Prognostics Data Repository (Saxena et al., 2008) (damage data used in this example correspond to laminate L1S19). A summary of the measurements of matrix micro-cracks used in this study is provided in Table 2.

5.4. Results

For predicting the estimate end of life (EOL) of the laminate, we are interested in computing the time when the damage grows beyond a predefined damage threshold. In this study, a threshold value of $\rho = 424$ cracks per meter is considered, hence $b = 424$. A total amount of $N = 100$ particles trajectories are employed for Algorithm 1 which are further used as initialization samples for Algorithm 3. The results of Algorithm 3 are presented for three different simulation levels ($m = 3$) in Figure 3a, by using $P_0 = 0.2$ and $M = 2.4 \cdot 10^4$

Table 1. Prior information and nominal values of main parameters used in calculations. Classical laminate theory may be used from these parameters to obtain the values of the remaining parameters attributable to the laminate configuration.

Type	Parameter	Nominal value	Units	COV (%)	Prior PDF
Mechanical	E_x	127.55	GPa	10	LN
	E_y	8.41	GPa	10	LN
	G_{xy}	6.20	GPa	10	LN
	$\frac{G_m}{d_0}$	$1 \cdot 10^5$	GPa/m	50	LN
	ν_{xy}	0.31	–	10	LN
	G_{yz}	2.82	GPa	10	LN
	h	$1.5 \cdot 10^{-4}$	m	10	LN
Fitting	α	1.80	–	20	LN
	A	$1 \cdot 10^{-4}$	–	20	LN
Errors	$\sigma_{v_{1_n}}$	4	$\frac{\#\text{ cracks}}{m\cdot\text{cycle}}$	–	$U(0.5, 8)$
	$\sigma_{v_{2_n}}$	0.01	$\frac{\#\text{ cracks}}{m\cdot\text{cycle}}$	–	$U(0.001, 0.02)$

Table 2. Experimental sequence of damage for cross-ply $[0_2/90_4]_s$ Torayca T700 CFRP laminate taken from the Composite dataset, NASA Ames Prognostics Data Repository (Saxena et al., 2008). The data are presented for micro-cracks density (ρ_n corresponding to specimen L1S19 in the dataset.)

Fatigue cycles, n	10^1	10^2	10^3	10^4	$2{\cdot}10^4$	$3{\cdot}10^4$	$4{\cdot}10^4$	$5{\cdot}10^4$	$6{\cdot}10^4$	$7{\cdot}10^4$	$8{\cdot}10^4$	$9{\cdot}10^4$	10^5
ρ_n [# cracks/m]	98.2	111.0	117.4	208.5	269.6	305.0	355.5	396.4	402.3	402.1	407.0	418.5	424.5
D_n	0.954	0.939	0.930	0.924	0.902	0.899	0.888	0.881	0.896	0.872	0.877	0.885	0.880

samples per simulation level. The results shown in Figure 3 are satisfactory in the sense that our algorithm has the ability to estimate the EOL with high precision with a moderate computational cost.

Figure 3b shows the EOL estimate by a histogram representation. The estimate is calculated by using the set of M samples from the latest subset ($\mathcal{F}_3$), which contributes in obtaining a higher quality of the estimate, as it is shown below.

6. DISCUSSION

To evaluate the computational improvement and accuracy that can be achieved using PFP-SubSim, the algorithm is compared with a standard PF-based prognostics algorithm in terms of efficiency in obtaining the EOL estimate. To this end, we examine the quality of an estimator based on samples from the different competing algorithms separately. Before proceeding with the analysis, we briefly review here general issues about quality of estimators.

Let $g(z_n) \geqslant b,\ n > k,\ n, k \in \mathbb{N}$ represents the fault indicator of our system, such that $P(z_t \in Z | g(z_t) \geqslant b) = \vartheta$, where ϑ is strictly higher than 0. By definition of T_{EOL}, the next equation also holds: $P(z_n \in Z | T_{EOL}(z_n) = 1) = \vartheta$, (see Section4). We want to obtain an estimator $\hat{\vartheta}$ from ϑ.

Suppose now that, starting at time $n > k$, N_{T2} samples of the joint state-parameter $\{z_n^{(v)}\}_{v=1}^{N_{T2}}$ are drawn from a state transition evolution model as in Eq. (1a) (or specifically Eq. (17), when the last two cited damage features in composites, are considered). By definition, $\{z_n^{(v)}\}$ are Markov chain samples of multi-step ahead predictions which are distributed with equally probability among N particle trajectories. The starting points of those trajectories are the latest N updated particles at time k, i.e. $\left\{ \left(z_k^{(i)} \right), \omega_k^{(i)} \right\}_{i=1}^{N}$, obtained using Algorithm 1, resulting in N independent Markov chains of fixed [4] length N_s. Hence $N_s = {}^{N_{T2}}/_{N}$.

It is straightforward that an unbiased estimator for ϑ can be readily obtained by simulating N i.i.d. trajectories of the process using Algorithm 2 and further compute the ratio of particles that reach the threshold b, as follows:

$$\vartheta \approx \hat{\vartheta} = \frac{1}{N_{T2}} \sum_{i=1}^{N} \sum_{q=1}^{N_s} T_{EOL}^{(i,q)} \tag{19}$$

where $T_{EOL}^{(i,q)}$ is the value of the T_{EOL} function evaluated at sample q of the ith Markov chain, i.e., $T_{EOL}^{(i,q)} = T_{EOL}(z_q^{(i)})$.

The coefficient of variation (c.o.v.) of the last estimator is given in Eq. (20) (the proof that Eq. (20) is the c.o.v. of $\hat{\vartheta}$ is given in the Appendix).

$$\delta_{\hat{\vartheta}} = \sqrt{\frac{(1-\vartheta)}{\vartheta N_{T2}} \left[1 + \gamma\right]} \tag{20}$$

In the last equation, γ is the autocorrelation factor, which is related with the level of correlation between the samples of any of the N Markov chains (see the Appendix).

[4] Only for this comparative exercise, Algorithm 2 is run using an "ad hoc" time threshold as stopping rule, instead of using a stopping rule based on exceedance of the particle trajectory over specified thresholds, as usual.

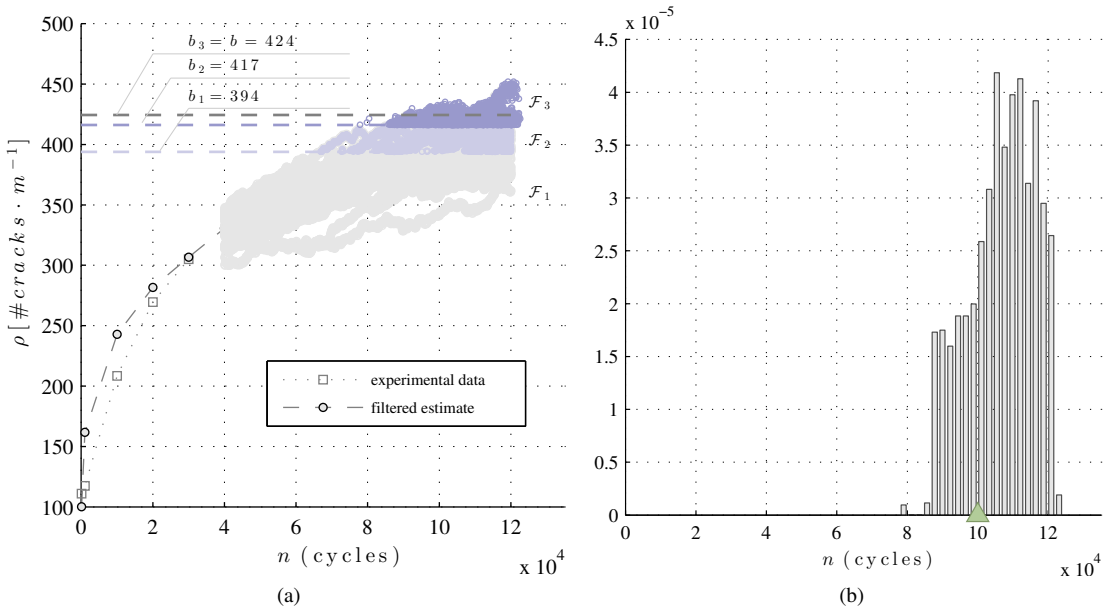

Figure 3. Prognostics results for predicting matrix micro-cracks density from cycle $n = 4 \cdot 10^4$ using the modified Paris' law model. (a): PFP-SubSim output using $M = 2.4 \cdot 10^4$ samples per simulation level. Each subset is defined by samples (circles) in the joint state-parameter space Z, where the latest intermediate predictive samples are marked in dark purple circles. (b): Histogram representation of the estimated EOL at cycle $n = 4 \cdot 10^4$. The green triangle represents the time (in cycles) when matrix micro-cracks density will reach the final threshold $b = 424$ $[\#cracks \cdot m^{-1}]$, which was reported in (Saxena et al., 2008) (laminate L1S19), and also shown in Table 2.

On the other hand, when Algorithm 3 is used for prognostics, an unbiased estimator from ϑ can be readily obtained as $\hat{\vartheta} = (P_0)^m$, where m is the total number simulation levels employed by the algorithm to reach the required threshold. The c.o.v. of $\hat{\vartheta}$ can be calculated as (see Zuev et al. for a detailed demonstration):

$$\delta_{\hat{\vartheta}} = \sqrt{\left(\frac{\log(\gamma)}{\log(P_0)}\right)^2 \frac{(1-P_0)}{P_0 N_{T3}}\,[1+\gamma]} \tag{21}$$

where N_{T3} is the total amount of evaluations employed by Algorithm 3.

Our objective for this comparative exercise is to demonstrate that Algorithm 3 is able to obtain the same, or better, quality of an EOL estimate but employing less model evaluations than Algorithm 2. For simplicity but no loss of generality, let us adopt a configuration in which both algorithms give samples with equal (or similar) level of correlation between them, hence γ is equal for both algorithms. It is reasonable to hypothesize that there exist a configuration for N_{T2} and N_{T3} in which both algorithms give the same quality for the EOL estimate. Then the next equation holds:

$$\frac{(1-P_0)(\log\vartheta)^2\vartheta N_{T2}}{(1-\vartheta)(\log P_0)^2 P_0 N_{T3}} = 1 \tag{22}$$

which is the result of dividing Eq. (21) by Eq. (20). From last equation, it is easy to obtain an expression for the number of samples N_{T2} required for Algorithm 2 to obtain an estimate of EOL with the same level of accuracy as that obtained using Algorithm 3, provided that a total amount of N_{T3} samples are employed:

$$N_{T2} = N_{T3}\,\underbrace{\frac{(1-\vartheta)P_0}{(1-P_0)\vartheta}\left(\frac{\log P_0^2}{\log\vartheta^2}\right)^2}_{\gg 1} \tag{23}$$

Observe that the factor that multiplies N_{T3} is always greater than unity, since by definition, $P_0 > \vartheta$. In rare-event problems (like asymptotic processes with conservative thresholds), $P_0 \gg \vartheta$, hence the last cited factor is fairly greater that 1, which demonstrates the high efficiency of our algorithm for prognostics of asymptotic processes.

As a numerical proof of the last postulate, the same exercise of prognostics for fatigue degradation is reproduced here although, in this case, by using the standard PF-based algorithm (Algorithm 2). The same total number of model evaluations as in Algorithm 3 is adopted, i.e. $N_{T2} = N_{T3} = 3 \times 2.4 \cdot 10^4 = 7.2 \cdot 10^4$, which are equally distributed among $N = 100$ particle trajectories. The results reveal that only 231 particles among a total amount of $7.2 \cdot 10^4$ particles reach

the threshold, in contrast to 2383 particles scrutinized when PFP-SubSim was employed. Since these particles serve to define the EOL sample size, a poorer EOL estimate is obtained when using Algorithm 2 and only a better estimate may be obtained by employing more simulations, which necessarily increases the computational cost. These results suggest that high efficiency can be gained by employing the PFP-SubSim algorithm for prognostics of asymptotic processes.

7. CONCLUSION

A new algorithm for PF-based prognostics has been presented in this paper. The algorithm combines the prognostics principles with the Subset Simulation method to achieve efficiency for simulating asymptotic processes. We demonstrate the computational efficiency and accuracy that can be gained with the novel algorithm in a case study about predicting the saturation of matrix micro-cracks due to fatigue damage in composites, that illustrate some of the challenges in a real-world application of the algorithm. The main conclusions of this work are:

- PFP-SubSim gets efficiency by adaptively simulating samples over a nested sequence of subsets until the final prognostic threshold is reached. The sequence of subset are adopted in an automated manner, which avoids tedious preliminary calibrations.
- For the case study considered, PFP-SubSim outperforms the standard PF-based prognostic algorithm, typically used by the prognostic community. It is demonstrated that PFP-SubSim is able to obtain the same quality of an EOL estimator by employing significant less evaluations.
- More research effort is required to formally explore the optimal calibration aspects of the algorithm using a variety of examples of application.

ACKNOWLEDGMENT

The two first authors would like to thank the Ministry of Education of Spain for the FPU grants AP2009- 4641, AP2009-2390, the European Union for project GGI3000IDIB and the Prognostics Center of Excellence at NASA Ames Research Center, which kindly hosted them during the course of this work. They would also like to thank Prof. James L. Beck from California Institute of Technology for the valuable guidance through Subset Simulation method. Authors would also like to thank the Structures and Composites lab at Stanford University for experimental data and NASA ARMD/AvSafe project SSAT, which provided partial support for this work.

NOMENCLATURE AND BASIC RELATIONS

The next are nomenclature description and basic relations to help understand the case study presented here (Section 5.1).

h	Ply thickness
h_{90}	$[90_n]$-sublaminate half-thickness
h_ϕ	$[\phi_{\frac{n_\phi}{2}}]$-sublaminate thickness
λ	Ply thickness ratio $\lambda = {}^{h_\phi}/_{h_{90}}$
$\bar{l}$	Average dimensionless half spacing of cracks, $\bar{l} = \frac{l}{h_{90}}$
E_x^{90}	Undamaged x-direction $[90_n]$ sublaminate modulus
$E_{x,0}$	Undamaged x-direction laminate Young's modulus
E_x^*	Damaged x-direction laminate Young's modulus
$E_x^{(\phi)}$	Longitudinal Young's modulus
$E_y^{(\phi)}$	Transverse Young's modulus
$\nu_{xy}^{(\phi)}$	In-plane Poisson ratio
σ_x	Maximum applied stress

The function a in Eq. (12) can is expressed as a function of the laminate and ply properties listed above as:

$$a = \frac{E_y h_{90}}{E_x h_\phi}\left(1 - \nu_{xy}^{(\phi)} \frac{\frac{\nu_{xy}^{(\phi)} h_{90}}{E_y^{(\phi)}} + \frac{\nu_{xy} h_\phi}{E_y}}{\frac{h_{90}}{E_y^{(\phi)}} + \frac{h_\phi}{E_x}}\right) \frac{1 - \nu_{xy}\nu_{xy}^{(\phi)}}{1 - \nu_{xy}^2 \frac{E_y}{E_x}} \tag{24}$$

REFERENCES

Arulampalam, M. S., Maskell, S., Gordon, N., & Clapp, T. (2002). A tutorial on particle filters for online nonlinear/non-Gaussian Bayesian tracking. *Signal Processing, IEEE Transactions on*, *50*(2), 174–188.

Au, S., & Beck, J. (2001). Estimation of small failure probabilities in high dimensions by Subset Simulation. *Probabilistic Engineering Mechanics*, *16*(4), 263–277.

Au, S., & Beck, J. (2003). Subset Simulation and its application to seismic risk based on dynamic analysis. *Journal of Engineering Mechanics*, *129*(8), 901-917.

Beck, J. (2010). Bayesian system identification based on probability logic. *Structural Control and Health Monitoring*, *17*(7), 825–847.

Cappe, O., Guillin, A., Marin, J., & Robert, C. (2004). Population Monte Carlo. *Journal of Computational and Graphical Statistics*, *13*(4), 907-927.

Chiachío, M., Chiachío, J., Saxena, A., Rus, G., & Goebel, K. (2013). Fatigue damage prognosis in FRP composites by combining multi-scale degradation fault modes in an uncertainty Bayesian framework. In *Proceedings of Structural Health Monitoring, 2013* (Vol. 1).

Chiachío, J., Chiachío, M., Saxena, A., Rus, G., & Goebel, K. (2013). An energy-based prognostics framework to predict fatigue damage evolution in composites. In *Proceedings of the Annual Conference of the Prognostics and Health Management Society, 2013* (Vol. 1, pp. 363–371).

Ching, J., Au, S., & Beck, J. (2005). Reliability estimation of dynamical systems subject to stochastic excitation using Subset Simulation with splitting. *Com-*

puter Methods in Applied Mechanics and Engineering, *194*(12-16), 1557–1579.

Daigle, M., & Goebel, K. (2011). Multiple damage progression paths in model-based prognostics. In *Aerospace conference, 2011* IEEE (pp. 1–10).

Garrett, K., & Bailey, J. (1977). Multiple transverse fracture in 90° cross-ply laminates of a glass fibre-reinforced polyester. *Journal of Materials Science*, *12*(1), 157–168.

Gordon, N., Salmond, D., & Smith, A. (1993). Novel approach to nonlinear/non-Gaussian Bayesian state estimation. *IEEE-Proceedings-F*, *140*, 107–113.

Gudmundson, P., & Weilin, Z. (1993). An analytic model for thermoelastic properties of composite laminates containing transverse matrix cracks. *International Journal of Solids and Structures*, *30*(23), 3211–3231.

Hashin, Z. (1985). Analysis of cracked laminates: a variational approach. *Mechanics of Materials*, *4*(2), 121–136.

Highsmith, A., & Reifsnider, K. (1982). Stiffness-reduction mechanisms in composite laminates. *Damage in composite materials, ASTM STP*, *775*, 103–117.

Joffe, R., & Varna, J. (1999). Analytical modeling of stiffness reduction in symmetric and balanced laminates due to cracks in 90 layers. *Composites Science and Technology*, *59*(11), 1641–1652.

Larrosa, C., & Chang, F. (2012). Real time in-situ damage classification, quantification and diagnosis for composite structures. In *Proceedings of the 19th* I*nternational* C*ongress on* S*ound and* V*ibration* (Vol. 15).

Lundmark, P., & Varna, J. (2005). Constitutive relationships for laminates with ply cracks in in-plane loading. *International Journal of Damage Mechanics*, *14*(3), 235–259.

Metropolis, N., Rosenbluth, A., Rosenbluth, M., Teller, A., & Teller, E. (1953). Equation of state calculations by fast computing machines. *The journal of chemical physics*, *21*, 1087–1092.

Nairn, J., & Hu, S. (1992). The initiation and growth of delaminations induced by matrix microcracks in laminated composites. *International Journal of Fracture*, *57*(1), 1–24.

Nairn, J. A. (1989). The strain energy release rate of composite microcracking: a variational approach. *Journal of Composite Materials*, *23*(11), 1106–1129.

Nairn, J. A. (1995). Some new variational mechanics results on composite microcracking. In *Proc. 10th international conference on composite materials (iccm-10) whistler bc, canada.*

Orchard, M., Kacprzynski, G., Goebel, K., Saha, B., & Vachtsevanos, G. (2008). Advances in uncertainty representation and management for particle filtering applied to prognostics. In *International conference on prognostics and health management.*

Rubin, D. (1987). A noniterative sampling/importance resampling alternative to the data augmentation algorithm for creating a few imputations when the fraction of missing information is modest: the SIR algorithm (discussion of tanner and wong). *Journal of American Statistical Association*, *82*, 543–546.

Saltelli, A., Ratto, M., Andres, T., Campolongo, F., Cariboni, J., Gatelli, D., ... Tarantola, S. (2008). *Global sensitivity analysis: The primer*. Wiley-Interscience.

Sankararaman, S., & Goebel, K. (2013). Uncertainty quantification in remaining useful life of aerospace components using state space models and inverse FORM. In *AIAA, ASME, ASCE, AHS, ASC, Structures, Structural Dynamics, and materials conference* (pp. 1–10). AIAA.

Saxena, A., Goebel, K., Larrosa, C., & Chang, F. (2008). *CFRP Composites dataset.* (NASA Ames Prognostics Data Repository, [http://ti.arc.nasa.gov/project/prognostic-data-repository], NASA Ames, Moffett Field, CA)

Saxena, A., Goebel, K., Larrosa, C., Janapati, V., Roy, S., & Chang, F. (2011). Accelerated aging experiments for prognostics of damage growth in composites materials. In *The 8th International Workshop on Structural Health Monitoring, F.-K. Chang, editor.* (Vol. 15).

Zuev, K., Beck, J., Au, S., & Katafygiotis, L. (2011). Bayesian post-processor and other enhancements of Subset Simulation for estimating failure probabilities in high dimensions. *Computers & Structures*, *93*, 283-296.

BIOGRAPHIES

Manuel Chiachío is a PhD Candidate at the Department of Structural Mechanics, University of Granada, Spain. His research focus on uncertainty quantification of fatigue damage in composites using Bayesian methods. He holds a Masters of Science in Civil Engineering (2007) and a Master of Science in Structural Engineering (2011), at the University of Granada. Prior to joining the University of Granada in 2011, Juan worked as a structural engineer in "Sener Ingenieria y Sistemas, S.A", since 2007. His research has been awarded by the National Council of Education through one of the prestigious FPU fellowships, by the Andalusian Society of promotion of the Talent and by the European Council of Civil Engineers (ECCM) with the Silver Medal prize in the 1st European Contest of Structural Design (2008). During the course of his PhD work, Manuel has worked as guest scientist at world-class universities and institutions, like Technical University of Hamburg (Germany), California Institute of Technology (Caltech) and NASA Ames Research Center (USA).

Juan Chiachío is a PhD Candidate at the Department of Structural Mechanics, University of Granada, Spain. His research

focus on uncertainty quantification of fatigue damage in composites using Bayesian methods. He holds a Masters of Science in Civil Engineering (2007) and a Master of Science in Structural Engineering (2011), at the University of Granada. Prior to joining the University of Granada in 2011, Juan worked as a structural engineer in "Sener Ingenieria y Sistemas, S.A", since 2007. His research has been awarded by the National Council of Education through one of the prestigious FPU fellowships, by the Andalusian Society of promotion of the Talent and by the European Council of Civil Engineers (ECCM) with the Silver Medal prize in the 1st European Contest of Structural Design (2008). During the course of his PhD work, Juan has worked as guest scientist at world-class universities and institutions, like Technical University of Hamburg (Germany), California Institute of Technology (Caltech) and NASA Ames Research Center (USA).

Guillermo Rus started his research on computational mechanics at the University of Granada (UGR, 1995), where he disputed the PhD thesis on Numerical Methods for Nondestructive Identification of Defects (2001). He applied these experimentally at the NDE Lab at MIT (USA) as a Fulbright Postdoctoral Fellow, rendering novel robust quantitative approaches to ultrasonics monitoring. He started up the NDE Lab at the UGR (`www.ugr.es/ endlab`) as assistant professor in 2003, focusing on bioengineering applications in collaboration with University College London, Universit Paris VI and the Nanomaterials Technology Lab. (Spain), among others. He is also transferring this diagnosis technology to civil engineering for monitoring structural health of advanced materials, such as FRP damage state monitoring. Rus tenured as associate professor in 2009 at UGR, is the author of 30 SCI papers, 9 books chapters, 3 patents and 18 invited seminars. His research career has been awarded by the Juan Carlos Simo prize for young researchers (Spain, 2007), the Honorary Fellowship of the Wessex Institute of Technology (UK, 2005), Fulbright Fellowship (USA, 2002) and the Excellence PhD award (Granada, 2001).

Abhinav Saxena is a Research Scientist with SGT Inc. at the Prognostics Center of Excellence of NASA Ames Research Center, Moffett Field CA. His research focus lies in developing and evaluating prognostic algorithms for engineering systems using soft computing techniques. He has co-authored more than seventy technical papers including several book chapters on topics related to PHM. He is also a member of the SAE's HM-1 committee on Integrated Vehicle Health Management Systems and IEEE working group for standards on prognostics. Abhinav is editor-in-chief of the International Journal of PHM and has led technical program committees in several PHM conferences. He is also a SGT technical fellow for prognostics. He has a PhD in Electrical and Computer Engineering from Georgia Institute of Technology, Atlanta. He earned his B.Tech in 2001 from Indian Institute of Technology (IIT) Delhi, and Masters Degree in 2003 from Georgia Tech. He has been a GM manufacturing scholar and is also a member of several professional societies including PHM Society, SAE, IEEE, AIAA, and ASME.

Kai Goebel is Deputy Area Lead of the Discovery and Systems Health Technology Area at NASA Ames Research Center. He also coordinates the Prognostics Center of Excellence. Prior to joining NASA in 2006, he was a senior research scientist at General Electric Corporate Research and Development center since 1997. Dr. Goebel received his Ph.D at the University of California at Berkeley in 1996. He has carried out applied research in the areas of real time monitoring, diagnostics, and prognostics and he has fielded numerous applications for aircraft engines, transportation systems, medical systems, and manufacturing systems. He holds 17 patents and has co-authored more than 250 technical papers in the field of IVHM. Dr. Goebel was an adjunct professor of the CS Department at Rensselaer Polytechnic Institute (RPI), Troy, NY, between 1998 and 2005 where he taught classes in Soft Computing and Applied Intelligent Reasoning Systems. He has been the co-advisor of 6 Ph.D. students. Dr. Goebel is a member of several professional societies, including ASME, AAAI, AIAA, IEEE, VDI, SAE, and ISO. He was the General Chair of the Annual Conference of the PHM Society, 2009, has given numerous invited and keynote talks and held many chair positions at the PHM conference and the AAAI Annual meetings series. He is currently member of the board of directors of the PHM Society and associate editor of the International Journal of PHM.

APPENDIX

Let $T_{EOL}^{(i,q)}$ be the threshold function as defined in Section 2.1 and applied for the qth sample in the ith Markov chain, i.e. $T_{EOL}^{(i,q)} = T_{EOL}\big(z_{(i,q)}\big)$, $i = 1, \ldots, N$, $q = 1, \ldots N_s$. Observe that $T_{EOL}^{(i,q)}$ is a Bernoulli random variable of parameter ϑ. It is straightforward to obtain an unbiased estimator for ϑ by simulating N i.i.d. trajectories of the process and further compute the ratio of particles that reach the threshold b, as follows:

$$\vartheta \approx \hat{\vartheta} = \frac{1}{N_{T2}} \sum_{i=1}^{N} \sum_{q=1}^{N_s} T_{EOL}^{(i,q)} \tag{25}$$

where $T_{EOL}^{(i,q)}$ is the qth Bernoulli trial at trajectory i. The variance of $\hat{\vartheta}$ can be calculated as:

$$\mathrm{Var}\left[\hat{\vartheta}\right] = \mathbb{E}\left[\hat{\vartheta} - \vartheta\right]^2 = \mathbb{E}\left[\frac{1}{N_{T2}} \sum_{i=1}^{N} \sum_{q=1}^{N_s} \big(T_{EOL}^{(i,q)} - \vartheta\big)\right]^2$$
$$\frac{1}{N_{T2}} \sum_{i=1}^{N} \underbrace{\mathbb{E}\left[\sum_{q=1}^{N_s} (T_{EOL}^{(i,q)} - \vartheta)\right]^2}_{(*)} \tag{26}$$

Note that (*) can be evaluated by means of the autocovariances of the stationary sequence $T_{EOL}^{(i,q)}$, $q = 1, \ldots, N_s$, as:

$$\mathbb{E}\left[\sum_{q=1}^{N_s}(T_{EOL}^{(i,q)} - \vartheta)\right]^2 = \sum_{q,l=1}^{N_s} \varphi^{(i)}(l) \tag{27}$$

where $\varphi^{(i)}(l)$ is the autocovariance of the ith chain at lag l from q, i.e., $\varphi^{(i)}(l) = \mathbb{E}\left[T_{EOL}^{(i,q)})T_{EOL}^{(i,q+l)})\right] - \vartheta^2$, $l = 1, \ldots, N_s$. In the last equation, it is assumed that each trajectory is probabilistically equivalent, which is motivated by the use of PF with sequential importance resampling (SIR), as in Algorithm 1. Therefore, we will use the term $\varphi(l)$ with independence of the chain index i.

Next, we evaluate Eq. (27):

$$\sum_{q,l=1}^{N_s} \varphi(l) = N_s\varphi(0) + 2\sum_{l=1}^{N_s-1}(N_s - q)\varphi(l) \tag{28}$$

and substitute Eq. (28) into Eq. (26):

$$\text{Var}\left[\hat{\vartheta}\right] = \frac{\varphi(0)}{N_{T2}}\left[1 + \underbrace{2\sum_{l=1}^{N_s-1}\left(\frac{N_s - l}{N_s}\right)\frac{\varphi(l)}{\varphi(0)}}_{\gamma}\right] \tag{29}$$

Note that $\varphi(0)$ is the variance of any ith Markov chain $T_{EOL}^{(i,q)}$), which is compounded by Bernoulli trials of parameter ϑ, hence $\varphi(0) = \text{Var}\left[T_{EOL}^{(i,q)}\right] = \vartheta(1-\vartheta)$, $q = 1, \ldots, N_s$. Equation (29) can be expressed in a simplified manner, as:

$$\text{Var}\left[\hat{\vartheta}\right] = \frac{\vartheta(1-\vartheta)}{N_{T2}}\left[1 + \gamma\right] \tag{30}$$

where γ is a correlation factor who penalizes the quality of the estimator when highly correlated samples for the Markov chains are employed. Note that, in model-based prognostics, the value of γ is directly related with the efficiency of the *artificial dynamics* in drawing samples in $\mathbf{\Theta}$ although it is not explicitly reflected here, since each Bernoulli trial is previously sampled from $p(\theta_t|\theta_{t-1})$ (see Algorithm 2). An study of the influence of the γ is out of the scope of this work.

Finally, the c.o.v. of $\hat{\vartheta}$, $\delta_{\hat{\vartheta}}$, is expressed as shown bellow:

$$\delta_{\hat{\vartheta}} = \sqrt{\frac{(1-\vartheta)}{\vartheta N_{T2}}\left[1 + \gamma\right]} \tag{31}$$